


Trapping Ion Coulomb Crystals in an Optical Lattice

Daniel Hoenig¹, Fabian Thielemann¹, Leon Karpa^{1,2}, Thomas Walker¹, Amir Mohammadi¹, and Tobias Schaez^{1,*}
¹*Albert-Ludwigs-Universität Freiburg, Physikalisches Institut, 79104 Freiburg, Germany*
²*Leibniz Universität Hannover, Institut für Quantenoptik, 30167 Hannover, Germany*

 (Received 20 June 2023; revised 14 November 2023; accepted 12 February 2024; published 29 March 2024)

We report the optical trapping of multiple ions localized at individual lattice sites of a one-dimensional optical lattice. We observe a fivefold increased range of axial dc-electric field strength for which ions can be optically trapped with high probability and an increase of the axial eigenfrequency by 2 orders of magnitude compared to an optical dipole trap without interference but of similar intensity. Our findings motivate an alternative pathway to extend arrays of trapped ions in size and dimension, enabling quantum simulations with particles interacting at long range.

DOI: 10.1103/PhysRevLett.132.133003

Analog quantum simulation—exploiting well controlled quantum systems to experimentally simulate phenomena in nature, which are otherwise hard to access—has seen great success with the emergence of several well-controlled experimental platforms [1–5]. However, it remains an outstanding objective to explore the regime beyond efficient numerical tractability, for example, by addressing the class of problems incorporating interaction at long range while exceeding one dimension [2]. Promising approaches include extending the interaction range between optically trapped neutral particles by employing strongly dipolar (Rydberg) atoms [6,7] or molecules [8] or using multi-species atomic ensembles coupled to cavities [9].

Trapping ion Coulomb crystals (CCs) in radiofrequency (rf) traps allows the direct exploitation of the long range Coulomb interaction [10,11]. Experiments with linear CCs have led to seminal results (see Refs. [12–14] and references therein). Yet, extending the approach to two- or three-dimensional CCs in linear rf traps enforces a spatial displacement of the ions from the rf node, causing an rf-driven motion, the so called excess micromotion. Aligning the orientation of the interaction perpendicular to the micromotion, could substantially reduce the impact for some applications [15–17]. Still, already in few ion CCs, the kinetic energy of the synchronized micromotion exceeds the thermal energy by several orders of magnitude, similar to the approach in Penning traps [11]. Trapping ions in arrays of individual rf surface traps mitigates the micromotion in higher dimensions, and permits single site control [18–23]. However, extending the size of the arrays, while maintaining sufficiently small electrode structures, remains a challenge. Hybrid traps, replacing the axial confinement in rf traps by a 1D optical lattice, were successfully employed to axially pin ions by the light field [24–27]. This has been used to simulate friction in one dimension on an atomic scale [28–32] and was proposed as

a platform to study structural phase-transitions in two dimensions [33].

Optical trapping of CCs, i.e., in absence of any rf fields, offers a possibility to extend arrays of ions in size and dimension. First, micromotion is negligible for optically trapped ions [34]. Second, optical fields allow the realization and dynamic control of close to arbitrary potential landscapes, such as multidimensional microtrap arrays on the nanometer scale [35,36]. Finally, optical trapping allows for joint confinement of atoms and ions [37,38], potentially extending the quantum simulation toolbox to arrays of ions and (Rydberg) atoms [39–41]. Optical trapping of a single ion [42–44] as well as CCs [45,46] has been demonstrated for single-beam optical dipole traps (ODTs). Additionally, a single ion has been confined in a near-resonant optical lattice [47]. In this Letter, we demonstrate optical trapping of multiple ions in a far-detuned optical lattice, realizing single-site localization at individual lattice sites. We compare the eigenfrequencies of the ions in the lattice to those of ions in a noninterfering ODT and observe an increase of the axial eigenfrequency by 2 orders of magnitude.

A schematic representation of the experimental setup is given in Fig. 1(a). We initially trap CCs of $^{138}\text{Ba}^+$ ions in a linear segmented rf trap (trap axis defines the z axis) with secular frequencies $(\omega_x, \omega_y, \omega_z) \approx 2\pi \times (100, 100, 12)$ kHz at driving frequency $\Omega_{\text{rf}} = 2\pi \times 1.416$ MHz. The axial secular frequency ω_z receives contributions from the rf field ($\approx 2\pi \times 3$ kHz) as well as from additional dc confinement supplied by the outer segments, collectively forming the two end caps of the trap ($\omega_{z,\text{dc}} \approx 2\pi \times 11.5$ kHz). In this trap, the ions form a linear chain with an interion distance of ≈ 70 μm (60 μm) for $N = 2(3)$ ions. The axial dc confinement results in radial deconfinement along one of the radial modes [45], reducing the confinement to $\omega_x \approx \sqrt{\omega_{x,\text{rf}}^2 - \omega_{z,\text{dc}}^2}$. The ions experience a magnetic field

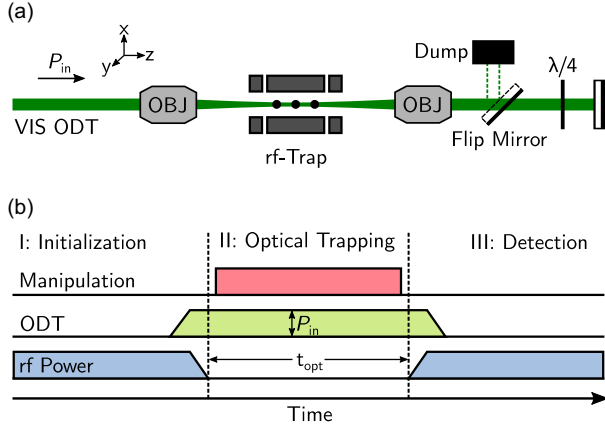


FIG. 1. Schematic representation of the experiment. (a) Setup (not to scale): The setup consists of a linear rf trap with segmented dc blades and an optical dipole trap. The ODT is generated by a linear polarized beam ($\lambda = 532$ nm) with power P_{in} , aligned along the common z axis. After the beam passes the trap, we either block it with a flip mirror, or retroreflect it, with the polarization of the retroreflection set with a quarter-wave plate. (b) Sketch of the experimental sequence: We prepare a linear Coulomb crystal in the rf trap (I: Initialization). We transfer the crystal into one of the ODT configurations (II: Optical trapping) and optionally act on the ions with additional fields. After the optical trapping duration t_{opt} , we detect remaining ions in the rf trap (III: Detection).

of approximately $300 \mu\text{T}$ at an angle of about 75° with respect to the z axis. We generate an ODT with a linear polarized laser at wavelength $\lambda = 532$ nm and power $P_{\text{in}} \in [0, 7.2]$ W aligned along the z axis. We focus the incident beam with a first objective to a beam waist ($1/e^2$ of intensity) of $w_{\text{in}} \approx 6.6 \mu\text{m}$ at the rf node, where we position the CCs' center of mass. After the beam passes the vacuum chamber, we collimate it with a second objective, before optionally retroreflecting and refocusing it on the ion with $P_{\text{ret}} \approx 0.86 \times P_{\text{in}}$ and a beam waist matching w_{in} within 10%. We realize three different ODT configurations, assisted by the axial dc confinement: (i) A single-beam-ODT, by blocking the incident beam with the flip mirror behind the chamber. (ii) A lin \perp lin-ODT, by rotating the polarization of the retroreflection by 90° with a quarter-wave plate. This results in a polarization gradient along the trap axis, modulating the optical potential [48]. (iii) A lin \parallel lin-ODT, obtained by overlapping the incident beam with a parallel polarized retroreflection. In this configuration the two beams interfere constructively, forming a 1D optical lattice.

Our optical trapping experiments consist of three phases [Fig. 1(b)]: In the initial phase, we load ions into the rf trap and laser cool them (D1-line) close to the Doppler temperature $T_{\text{D}} \approx 400 \mu\text{K}$ in all motional degrees of freedom [44]. We monitor the ions by fluorescence imaging, to prepare isotope-pure CCs of $N \leq 3$ ions in the $6S_{1/2}$ state as described in [49] and [46], and compensate stray fields

to $E_{\text{stray}} \leq 10 \text{ mV m}^{-1}$. For the second phase, we transfer the CC from the rf trap into the ODT. To this end, we increase P_{in} to its chosen value within $t_{\text{ramp}} \approx 100 \mu\text{s}$ and subsequently turn off the rf field (ringdown time of $32 \mu\text{s}$). During the optical trapping duration t_{opt} , we optionally manipulate the ions with electric control fields. In the final phase, we turn the rf trap on, switch the ODT off and detect remaining ions via fluorescence imaging. We register a CC as optically trapped, if all ions are detected and repeat the protocol for $n = 10$ to 20 times, to derive the optical trapping probability p_{opt} . As a measure of statistical uncertainty for p_{opt} we employ Wilson-Score 1σ intervals [50]. Currently, systematic effects prevent us from increasing n as well as from accumulating data from different experimental periods, in order to reduce statistical uncertainties. However, we verify that the observed features are not due to statistical fluctuations and show representative datasets.

In order to study the effect of the ODTs on the radial confinement of the ions, we investigate the radial motional eigenfrequencies $f_{\text{rad,exp}}$ of a single ion for the different configurations. To derive $f_{\text{rad,exp}}$, we sinusoidally modulate the voltage on one of the end caps during $t_{\text{opt}} = 1.5$ ms and measure p_{opt} in dependence on the modulation frequency f_{mod} . Tuning f_{mod} close to resonance, we find a reduction of p_{opt} due to coherent motional excitation. We compare the radial eigenfrequencies for the three ODT configurations at $P_{\text{in}} = 5.04$ and 6.30 W [Figs. 2(a) and 2(b), respectively]. The observed $f_{\text{rad,exp}}$ scale approximately with $\sqrt{P_{\text{in}}}$. Additionally, the measurements show a significant increase in radial confinement from the single-beam-ODT to the lin \perp lin-ODT and lin \parallel lin-ODT at a given P_{in} . We attribute the increase of $f_{\text{rad,exp}}$ in the lin \perp lin-ODT compared to the single-beam-ODT to the additional impact of P_{ret} , and the further increase in the lin \parallel lin-ODT to the interference of the beams. As a comparison, we estimate radial frequencies $f_{\text{rad,num}}$, based on a harmonic approximation of a numerically modeled trap potential. While all $f_{\text{rad,exp}}$ agree with their related $f_{\text{rad,num}}$ to within 1.5σ [51], they remain systematically below the $f_{\text{rad,num}}$ for the lin \perp lin and lin \parallel lin configurations. We attribute this systematic shift to our measurement method, which relies on exciting the ions to energies sufficient to escape the trap. The anharmonicity of the trapping potential and the related dependence of the ions' motional frequency on the oscillation amplitude leads to a higher rate of escape for f_{mod} initially detuned to the red. Finally, we consider contributions to the deviation by non-Gaussian ODT beams, as well as radial misalignment between the beams. For the lin \perp lin- and lin \parallel lin-ODT, the variation of the resonance widths between the different configurations, shown in Fig. 2, is comparable to the variation across different datasets for each configuration. We thus attribute the variation to systematic effects, such as drifts of the objectives and electric fields.

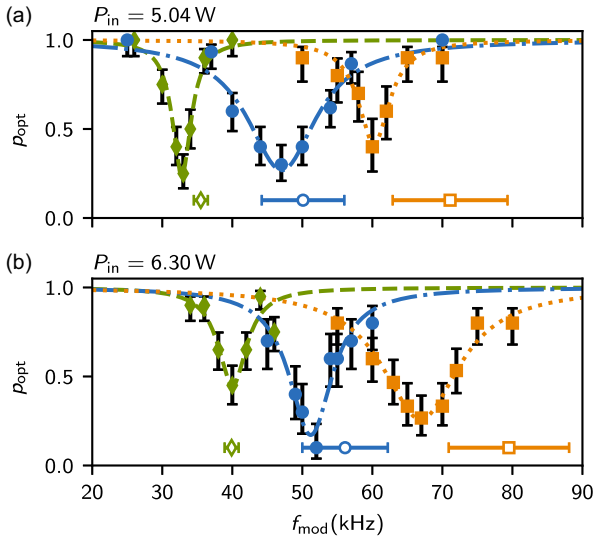


FIG. 2. Spectrometry of the radial modes of a single ion in different ODT configurations for (a) 5.04 and (b) 6.30 W. Shown is p_{opt} at different excitation frequencies f_{mod} for single beam (green diamonds), the lin \perp lin (blue circles), and the lin \parallel lin-ODT (orange squares). Lines depict Lorentzian fits to the data. Open symbols show numerical estimations for the resonance frequencies (error bars represent model uncertainties [51]).

To probe the axial confinement in the lin \parallel lin- and lin \perp lin-ODT, we measure p_{opt} for a single ion in dependence on a homogeneous axial electric field E_{ax} (Fig. 3). We compare the lin \parallel lin-ODT at $P_{\text{in}} = 3.25$ W to the lin \perp lin-ODT at $P_{\text{in}} = 6.30$ W. While this leads to comparable radial trap depths (≈ 17 mK), the expected axial depths of the individual trap sites differ. They are approximately

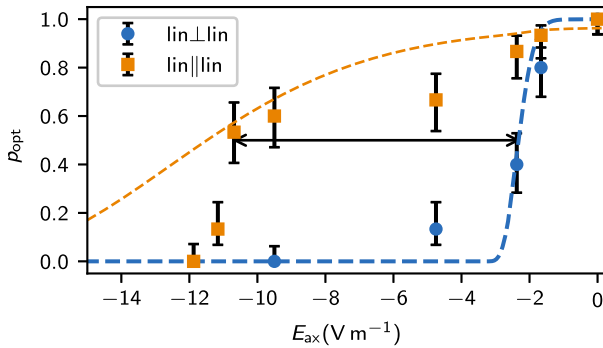


FIG. 3. Optical trapping probability p_{opt} for a single ion in the lin \perp lin- (blue circles) and lin \parallel lin-ODT (orange squares), exposed to an axial electric field E_{ax} . To reach comparable intensities in the two ODTs, we set P_{in} to 3.25 and 6.30 W, respectively. As the black arrow indicates, we can apply an approximately 5 times larger E_{ax} in the lin \parallel lin configuration, before p_{opt} decreases to 50%. The dashed blue curve shows the result of a simulation for ions with thermally distributed energy at temperature $T \approx 3 \times T_{\text{D}}$, neglecting any axial confinement by the light field. The orange dashed curve represents a simulated result for an initially optically single-site confined ion at $T \approx 6 \times T_{\text{D}}$.

3 mK for the lin \perp lin- and 22 mK for the lin \parallel lin-ODT. During t_{opt} , we increase E_{ax} within 200 μs to its dedicated value and keep it for 500 μs . We find p_{opt} enhanced for the lin \parallel lin configuration at $E_{\text{ax}} \geq 2 \text{ V m}^{-1}$ allowing the application of a 5 times larger E_{ax} before p_{opt} decreases to 50%. Since the radial confinement in both configurations is comparable, we attribute this difference in robustness of p_{opt} against E_{ax} to a difference in axial confinement. We compare the measured p_{opt} with the results of two simulations assuming thermally distributed kinetic energy E_{kin} with temperature T ; one accounting for axial confinement by the light field, the other neglecting it [51]. For the lin \perp lin-ODT we find good qualitative agreement with the experiment for $T \approx 3 \times T_{\text{D}}$, without the inclusion of axial optical confinement. We therefore do not find evidence for axial optical confinement, suggesting a nonthermal and strongly anisotropic energy distribution, with axial kinetic energies larger than the modulation depth due to the polarization gradient. To reproduce the enhanced p_{opt} in the lin \parallel lin-ODT, however, we have to include axial optical confinement and derive $T \approx 6 \times T_{\text{D}}$. We thus attribute the increased robustness of p_{opt} against E_{ax} to the enhancement of the axial restoring force by the interference of the beams, confining the ion at a single lattice site. The increase of kinetic energy is likely caused by (i) a nonadiabatic trap transfer, inducing axial (radial) excitations, (ii) crossing of radial rf trap instabilities during rf ramp down [58] and (iii) resonant axial excitation by the rf field during the transfer into the lin \perp lin- and lin \parallel lin-ODT. The increase in T suggests a further increased motional excitation during the transfer into the lin \parallel lin-ODT. Apart from the imperfections discussed above, we suspect a residual misalignment of E_{ax} , causing a decrease of the radial trap depth with increased E_{ax} . Additionally, we expect a nonthermal energy distribution in the ODT, due to the energy increase during trap-transfer.

As an independent measure of the axial confinement in the lin \parallel lin-ODT, we derive the axial eigenfrequencies $f_{\text{ax,exp}}$ of a single ion for $P_{\text{in}} = 3.30$ W (6.30 W) [Fig. 4(a)]. During t_{opt} , we first apply a voltage offset on one of the end caps to generate $E_{\text{ax}} \approx 0.6 \text{ V m}^{-1}$ (0.9 V m^{-1}), before additionally modulating the voltage on the opposite end cap at frequency f_{mod} for 500 μs . E_{ax} is needed, since the modulation alone does not lead to a f_{mod} dependent reduction of p_{opt} . It is chosen small enough such that $p_{\text{opt}} \approx 1$ without the modulation. We attribute the need for the additional E_{ax} to the anharmonicity of the axial potential, inhibiting efficient resonant excitation at f_{mod} for increasing motional amplitudes. Similar to $f_{\text{rad,exp}}$, we observe a scaling of $f_{\text{ax,exp}} \sim \sqrt{P_{\text{in}}}$, evidencing that the measured confinement originates from the optical potential. Furthermore, the obtained $f_{\text{ax,exp}}$ are more than 2 orders of magnitude larger than the axial frequency in the single-beam ODT where the confinement is dominated by the dc field. This increase

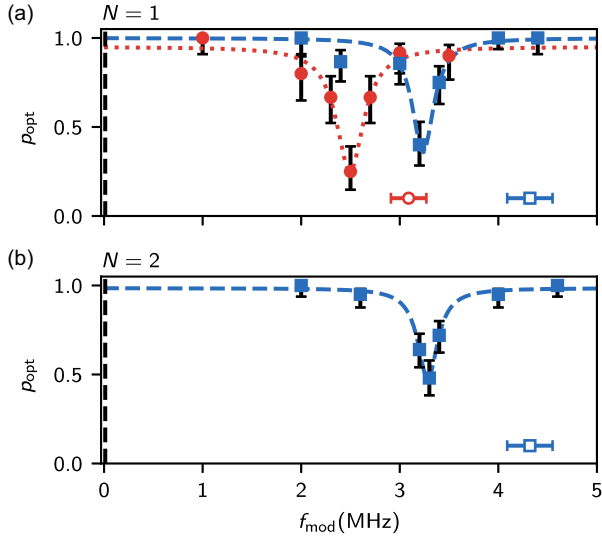


FIG. 4. Spectrometry of the axial eigenfrequencies in the lin||lin-trap for (a) a single ion and (b) a two ion crystal. The measurements were performed at $P_{\text{in}} = 3.30$ (red circles) and $P_{\text{in}} = 6.30$ W (blue squares). Shown is p_{opt} , in dependence on the frequency f_{mod} of an axial driving field. The dashed and dotted lines show the result of a Lorentzian fit to the data. Open symbols represent an estimation of the expected frequencies based on numerical calculations [51]. The observed frequencies are 2 orders of magnitude larger than the eigenfrequency measured for the single-beam-ODT, located at the dashed black line.

suggests that the ion is axially optically confined at a single lattice site. We repeat the measurement for $P_{\text{in}} = 6.30$ W, $E_{\text{ax}} \approx 0.6$ V m $^{-1}$, and a CC of $N = 2$ [Fig. 4(b)] (We perform this experiment at $P_{\text{in}} = 6.30$ W only, since $p_{\text{opt}} \ll 1$ for $P_{\text{in}} = 3.30$ W and additional E_{ax}). The agreement of $f_{\text{ax,exp}}$ for $N = 2$ and $N = 1$ at identical P_{in} shows, that the ions in the CC are initially axially confined within individual lattice sites. Using the same model as for $f_{\text{rad,num}}$, we derive numerical approximations $f_{\text{ax,num}}$. All $f_{\text{ax,exp}}$ remain at 80% (76%) of $f_{\text{ax,num}}$ for the 3.30 W (6.30 W) measurement. However the ratio between axial and radial frequencies agrees with the ratio of the numerical estimates within 1σ [51].

Finally, we trap CCs with $N = 1, 2, 3$ ions in the lin||lin-ODT for $t_{\text{opt}} = 500$ μs and measure the dependence of p_{opt} on P_{in} (Fig. 5). We achieve trapping of up to $N = 3$ in the lin||lin-trap with p_{opt} close to one. As N increases, we need considerably more power, to reliably trap the CCs. While for $N > 1$, the beam divergence and mutual Coulomb repulsion between the ions reduce the potential depth, this reduction alone does not explain the observed reduction of p_{opt} for $N = 3$. We derive an estimate of the ion energies via the radial-cutoff model, assuming thermal distributions. Considering the reduced potential depths, it yields temperatures on the order of $(5, 10, 20) \times T_D$ for $N = 1, 2, 3$. We attribute this increase in ion temperature to the on average

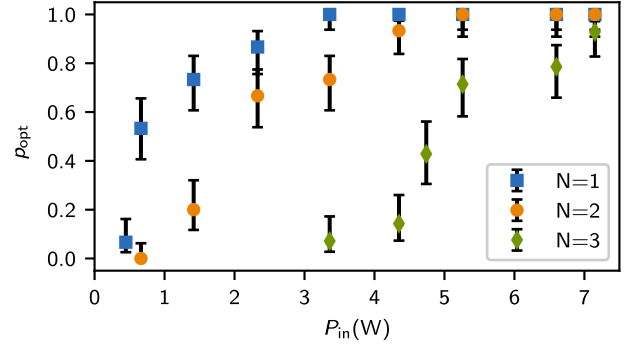


FIG. 5. Optical trapping probability p_{opt} for ion Coulomb crystals in the lin||lin trap with one (blue squares), two (orange circles), and three ions (green diamonds) in dependence on the incident beam power P_{in} . We achieve trapping of CCs of up to $N = 3$ ions with p_{opt} close to unity [$p_{\text{opt,max}}(N = 3) = 0.93_{-0.10}^{+0.04}$].

increased distance of ions from the axial rf node. As the rf field features an axial component increasing with distance to the rf node, this leads to an enhancement of E_{kin} for larger N during trap transfer.

In this Letter, we have shown that we can trap CCs with up to three ions in an optical lattice. In our measurements we observed the effect of excess heating during trap transfer, currently limiting us in the size of trappable CCs. By measuring the increased robustness of p_{opt} against axial displacement (see Fig. 3) and the axial eigenfrequencies of the ions in the lattice (see Fig. 4), we demonstrated that for $N \leq 2$ the ions are single-site confined at individual lattice sites even with increased kinetic energies.

One approach to mitigate the kinetic excitation during ODT loading is an improved adiabatic transfer—for example, via an intermittent single-beam-ODT, eventually building up the lattice with a second, individually controlled beam [47]. An alternative is to *in situ* ionize optically trapped neutral atoms, achieving small recoil energies by employing near-threshold photoionization or field ionization of Rydberg states [59,60]. Additionally, this would allow the interion distance to be reduced, while easing the loading process for higher-dimensional ensembles into lattices [40] or into optical-tweezer arrays with adjustable spacing [36]. To reach close to the motional ground state within individual lattice sites, we might exploit established sideband cooling schemes [26]. Alternatively, we could exploit sympathetic cooling via a bath of ultracold atoms [37,61]. This might enable continuous operation, since the electronic degree of freedom is not involved. However, even at reduced temperatures, an increased laser power might be required, to extend the ensemble. This can be assisted by the use of optical cavities [62,63] as demonstrated for optically trapped neutral atoms [64,65] and hybrid ion traps [25–27,29–32]. The ions could be imaged with fluorescence detection either *in situ* while Raman cooling [26] or free of effects induced by the ODT, by stroboscopically interleaving trapping and detection cycles.

Currently, offresonant scattering of photons from the ODT beams limits t_{opt} to a few milliseconds. The trapping durations could be enhanced by detuning the ODT, demonstrated for 1064 nm [44]. Using the $6S_{1/2} \rightarrow 5D_{5/2}$ transition [66] could then allow coherent control over the optical confinement, enabling the creation and study of coherent superpositions of structural crystal phases [67–69] and their entanglement. Providing higher-dimensional lattices, filled with neutral atoms and ions, could allow the investigation of novel aspects of atom-ion interaction, e.g., involving coherent charge transfer between lattice sites hosting either ions or atoms [39,41], the latter in circular Rydberg states [70]. Yet, the Coulomb interaction at long range comes along with mutual repulsion, limiting the filling factor of the lattice. However, the stiff confinement within the accessible optical landscape might permit us to address complex dynamics of interest, such as, the onset of Aharonov-Bohm physics via artificial gauge fields [71] or the experimental simulation of quantum-spin Hamiltonians [51], featuring spin frustration [72,73] and spin-glass dynamics [74].

The authors thank U. Warring for fruitful discussions and valuable input. This project has received funding from the European Research Council (ERC) under the European Union’s Horizon 2020 research and innovation program (Grant No. 648330) and the German Science Foundation (DFG) via SCHA 973/9-1. D. H. and F. T. acknowledge support from the German Science Foundation (DFG) within RTG 2717. A. M. and T. W. acknowledge additional support from the Georg H. Endress Foundation. L. K. acknowledges support from the German Science Foundation (DFG) via the Heisenberg program KA 4215/2-1.

* tobias.schaetz@physik.uni-freiburg.de

- [1] R. P. Feynman, Simulating physics with computers, *Int. J. Theor. Phys.* **21**, 467 (1982).
- [2] J. I. Cirac and P. Zoller, Goals and opportunities in quantum simulation, *Nat. Phys.* **8**, 264 (2012).
- [3] T. Schaetz, C. R. Monroe, and T. Esslinger, Focus on quantum simulation, *New J. Phys.* **15**, 085009 (2013).
- [4] I. M. Georgescu, S. Ashhab, and F. Nori, Quantum simulation, *Rev. Mod. Phys.* **86**, 153 (2014).
- [5] E. Altman *et al.*, Quantum simulators: Architectures and opportunities, *PRX Quantum* **2**, 017003 (2021).
- [6] S. Baier, M. J. Mark, D. Petter, K. Aikawa, L. Chomaz, Z. Cai, M. Baranov, P. Zoller, and F. Ferlaino, Extended Bose-Hubbard models with ultracold magnetic atoms, *Science* **352**, 201 (2016).
- [7] X. Wu, X. Liang, Y. Tian, F. Yang, C. Chen, Y.-C. Liu, M. K. Tey, and L. You, A concise review of Rydberg atom based quantum computation and quantum simulation, *Chin. Phys. B* **30**, 020305 (2021).
- [8] J. A. Blackmore, L. Caldwell, P. D. Gregory, E. M. Bridge, R. Sawant, J. Aldegunde, J. Mur-Petit, D. Jaksch, J. M. Hutson, B. E. Sauer, M. R. Tarbutt, and S. L. Cornish, Ultracold molecules for quantum simulation: rotational coherences in CaF and RbCs, *Quantum Sci. Technol.* **4**, 014010 (2018).
- [9] J. Argüello-Luengo, A. González-Tudela, T. Shi, P. Zoller, and J. I. Cirac, Analogue quantum chemistry simulation, *Nature (London)* **574**, 215 (2019).
- [10] R. C. Thompson, Ion Coulomb crystals, *Contemp. Phys.* **56**, 63 (2015).
- [11] M. Drewsen, Ion Coulomb crystals, *Physica (Amsterdam)* **460B**, 105 (2015).
- [12] R. Blatt and C. F. Roos, Quantum simulations with trapped ions, *Nat. Phys.* **8**, 277 (2012).
- [13] C. Schneider, D. Porras, and T. Schaetz, Experimental quantum simulations of many-body physics with trapped ions, *Rep. Prog. Phys.* **75**, 024401 (2012).
- [14] C. Monroe, W. C. Campbell, L.-M. Duan, Z.-X. Gong, A. V. Gorshkov, P. W. Hess, R. Islam, K. Kim, N. M. Linke, G. Pagano, P. Richerme, C. Senko, and N. Y. Yao, Programmable quantum simulations of spin systems with trapped ions, *Rev. Mod. Phys.* **93**, 025001 (2021).
- [15] M. D’Onofrio, Y. Xie, A. J. Rasmusson, E. Wolanski, J. Cui, and P. Richerme, Radial two-dimensional ion crystals in a linear Paul trap, *Phys. Rev. Lett.* **127**, 020503 (2021).
- [16] S.-T. Wang, C. Shen, and L.-M. Duan, Quantum computation under micromotion in a planar ion crystal, *Sci. Rep.* **5**, 8555 (2015).
- [17] D. Kiesenhofer, H. Hainzer, A. Zhdanov, P. C. Holz, M. Bock, T. Ollikainen, and C. F. Roos, Controlling two-dimensional Coulomb crystals of more than 100 ions in a monolithic radio-frequency trap, *PRX Quantum* **4**, 020317 (2023).
- [18] T. Schaetz, A. Friedenauer, H. Schmitz, L. Petersen, and S. Kahra, Towards (scalable) quantum simulations in ion traps, *J. Mod. Opt.* **54**, 2317 (2007).
- [19] J. Chiaverini and W. E. Lybarger, Laserless trapped-ion quantum simulations without spontaneous scattering using microtrap arrays, *Phys. Rev. A* **77**, 022324 (2008).
- [20] R. C. Sterling, H. Rattanasonti, S. Weidt, K. Lake, P. Srinivasan, S. C. Webster, M. Kraft, and W. K. Hensinger, Fabrication and operation of a two-dimensional ion-trap lattice on a high-voltage microchip, *Nat. Commun.* **5**, 3637 (2014).
- [21] M. Mielenz, H. Kalis, M. Wittemer, F. Hakelberg, U. Warring, R. Schmied, M. Blain, P. Maunz, D. L. Moehring, D. Leibfried, and T. Schaetz, Arrays of individually controlled ions suitable for two-dimensional quantum simulations, *Nat. Commun.* **7**, ncomms11839 (2016).
- [22] U. Warring, F. Hakelberg, P. Kiefer, M. Wittemer, and T. Schaetz, Trapped ion architecture for multi-dimensional quantum simulations, *Adv. Quantum Technol.* **3**, 1900137 (2020).
- [23] P. C. Holz, S. Aughter, G. Stocker, M. Valentini, K. Lakhmankiy, C. Rössler, P. Stampfer, S. Sgouridis, E. Aschauer, Y. Colombe, and R. Blatt, 2D linear trap array for quantum information processing, *Adv. Quantum Technol.* **3**, 2000031 (2020).
- [24] H. Katori, S. Schlipf, and H. Walther, Anomalous dynamics of a single ion in an optical lattice, *Phys. Rev. Lett.* **79**, 2221 (1997).

- [25] R. B. Linnet, I. D. Leroux, M. Marciante, A. Dantan, and M. Drewsen, Pinning an ion with an intracavity optical lattice, *Phys. Rev. Lett.* **109**, 233005 (2012).
- [26] L. Karpa, A. Bylinskii, D. Gangloff, M. Cetina, and V. Vuletić, Suppression of ion transport due to long-lived subwavelength localization by an optical lattice, *Phys. Rev. Lett.* **111**, 163002 (2013).
- [27] T. Lauprêtre, R. B. Linnet, I. D. Leroux, H. Landa, A. Dantan, and M. Drewsen, Controlling the potential landscape and normal modes of ion Coulomb crystals by a standing-wave optical potential, *Phys. Rev. A* **99**, 031401(R) (2019).
- [28] M. Cetina, A. Bylinskii, L. Karpa, D. Gangloff, K. M. Beck, Y. Ge, M. Scholz, A. T. Grier, I. Chuang, and V. Vuletić, One-dimensional array of ion chains coupled to an optical cavity, *New J. Phys.* **15**, 053001 (2013).
- [29] A. Bylinskii, D. Gangloff, and V. Vuletić, Tuning friction atom-by-atom in an ion-crystal simulator, *Science* **348**, 1115 (2015).
- [30] D. Gangloff, A. Bylinskii, I. Counts, W. Jhe, and V. Vuletić, Velocity tuning of friction with two trapped atoms, *Nat. Phys.* **11**, 915 (2015).
- [31] A. Bylinskii, D. Gangloff, I. Counts, and V. Vuletic, Observation of Aubry-type transition in finite atom chains via friction, *Nat. Mater.* **15**, 717 (2016).
- [32] D. A. Gangloff, A. Bylinskii, and V. Vuletić, Kinks and nanofriction: Structural phases in few-atom chains, *Phys. Rev. Res.* **2**, 013380 (2020).
- [33] P. Horak, A. Dantan, and M. Drewsen, Optically induced structural phase transitions in ion Coulomb crystals, *Phys. Rev. A* **86**, 043435 (2012).
- [34] C. Cormick, T. Schaetz, and G. Morigi, Trapping ions with lasers, *New J. Phys.* **13**, 043019 (2011).
- [35] D. Barredo, V. Lienhard, S. de Léséleuc, T. Lahaye, and A. Browaeys, Synthetic three-dimensional atomic structures assembled atom by atom, *Nature (London)* **561**, 79 (2018).
- [36] H. Bernien, S. Schwartz, A. Keesling, H. Levine, A. Omran, H. Pichler, S. Choi, A. S. Zibrov, M. Endres, M. Greiner, V. Vuletić, and M. D. Lukin, Probing many-body dynamics on a 51-atom quantum simulator, *Nature (London)* **551**, 579 (2017).
- [37] J. Schmidt, P. Weckesser, F. Thielemann, T. Schaetz, and L. Karpa, Optical traps for sympathetic cooling of ions with ultracold neutral atoms, *Phys. Rev. Lett.* **124**, 053402 (2020).
- [38] E. Perego, L. Duca, and C. Sias, Electro-optical ion trap for experiments with atom-ion quantum hybrid systems, *Appl. Sci.* **10**, 2222 (2020).
- [39] I. Lesanovsky, M. Müller, and P. Zoller, Trap-assisted creation of giant molecules and Rydberg-mediated coherent charge transfer in a Penning trap, *Phys. Rev. A* **79**, 010701 (R) (2009).
- [40] T. Schaetz, Trapping ions and atoms optically, *J. Phys. B* **50**, 102001 (2017).
- [41] R. Mukherjee, Charge dynamics of a molecular ion immersed in a Rydberg-dressed atomic lattice gas, *Phys. Rev. A* **100**, 013403 (2019).
- [42] C. Schneider, M. Enderlein, T. Huber, and T. Schaetz, Optical trapping of an ion, *Nat. Photonics* **4**, 772 (2010).
- [43] T. Huber, A. Lambrecht, J. Schmidt, L. Karpa, and T. Schaetz, A far-off-resonance optical trap for a Ba⁺ ion, *Nat. Commun.* **5**, 5587 (2014).
- [44] A. Lambrecht, J. Schmidt, P. Weckesser, M. Debatin, L. Karpa, and T. Schaetz, Long lifetimes and effective isolation of ions in optical and electrostatic traps, *Nat. Photonics* **11**, 704 (2017).
- [45] J. Schmidt, A. Lambrecht, P. Weckesser, M. Debatin, L. Karpa, and T. Schaetz, Optical Trapping of Ion Coulomb Crystals, *Phys. Rev. X* **8**, 021028 (2018).
- [46] P. Weckesser, F. Thielemann, D. Hoenig, A. Lambrecht, L. Karpa, and T. Schaetz, Trapping, shaping, and isolating of an ion Coulomb crystal via state-selective optical potentials, *Phys. Rev. A* **103**, 013112 (2021).
- [47] M. Enderlein, T. Huber, C. Schneider, and T. Schaetz, Single ions trapped in a one-dimensional optical lattice, *Phys. Rev. Lett.* **109**, 233004 (2012).
- [48] I. H. Deutsch and P. S. Jessen, Quantum-state control in optical lattices, *Phys. Rev. A* **57**, 1972 (1998).
- [49] J. Schmidt, D. Hönig, P. Weckesser, F. Thielemann, T. Schaetz, and L. Karpa, Mass-selective removal of ions from Paul traps using parametric excitation, *Appl. Phys. B* **126**, 176 (2020).
- [50] E. B. Wilson, Probable inference, the law of succession, and statistical inference, *J. Am. Stat. Assoc.* **22**, 209 (1927).
- [51] See Supplemental Material at <http://link.aps.org/supplemental/10.1103/PhysRevLett.132.133003> for detailed descriptions of the models and simulations, values of experimentally and numerically obtained resonance frequencies, as well as estimates regarding the extension of optically trapped Coulomb crystals in size and dimension and their suitability for quantum simulations of quantum spin Hamiltonians, which includes Refs. [52–57].
- [52] R. Grimm, M. Weidemüller, and Y. B. Ovchinnikov, Optical Dipole Traps for Neutral Atoms, in *Advances In Atomic, Molecular, and Optical Physics*, edited by B. Bederson and H. Walther (publisher Academic Press, New York, 2000), Vol. 42, pp. 95–170.
- [53] C. Schneider, M. Enderlein, T. Huber, S. Dürr, and T. Schaetz, Influence of static electric fields on an optical ion trap, *Phys. Rev. A* **85**, 013422 (2012).
- [54] A. Friedenauer, H. Schmitz, J. T. Glueckert, D. Porras, and T. Schaetz, Simulating a quantum magnet with trapped ions, *Nat. Phys.* **4**, 757 (2008).
- [55] D. Wineland, C. Monroe, W. Itano, D. Leibfried, B. King, and D. Meekhof, Experimental issues in coherent quantum-state manipulation of trapped atomic ions, *J. Res. Natl. Inst. Stand. Technol.* **103**, 259 (1998).
- [56] F. Hakelberg, P. Kiefer, M. Wittemer, U. Warring, and T. Schaetz, Interference in a prototype of a two dimensional ion trap array quantum simulator, *Phys. Rev. Lett.* **123**, 100504 (2019).
- [57] D. Porras and J. I. Cirac, Effective quantum spin systems with trapped ions, *Phys. Rev. Lett.* **92**, 207901 (2004).
- [58] R. Takai, K. Nakayama, W. Saiki, K. Ito, and H. Okamoto, Nonlinear resonance effects in a linear Paul trap, *J. Phys. Soc. Jpn.* **76**, 014802 (2007).
- [59] F. Engel, T. Dieterle, T. Schmid, C. Tomschitz, C. Veit, N. Zuber, R. Löw, T. Pfau, and F. Meinert, Observation of

- Rydberg Blockade induced by a single ion, *Phys. Rev. Lett.* **121**, 193401 (2018).
- [60] T. Dieterle, M. Berngruber, C. Hölzl, R. Löw, K. Jachymski, T. Pfau, and F. Meinert, Inelastic collision dynamics of a single cold ion immersed in a Bose-Einstein condensate, *Phys. Rev. A* **102**, 041301(R) (2020).
- [61] P. Weckesser, F. Thielemann, D. Wiater, A. Wojciechowska, L. Karpa, K. Jachymski, M. Tomza, T. Walker, and T. Schaetz, Observation of Feshbach resonances between a single ion and ultracold atoms, *Nature (London)* **600**, 429 (2021).
- [62] O. Wipfli, H. F. Passagem, C. Fischer, M. Grau, and J. P. Home, Integration of a high finesse cryogenic build-up cavity with an ion trap, *Rev. Sci. Instrum.* **94**, 083204 (2023).
- [63] Z. Sun, Y. H. Teoh, F. Rajabi, and R. Islam, Investigations of 2D ion crystals in a hybrid optical cavity trap for quantum information processing, *arXiv:2308.09231*.
- [64] H. Ritsch, P. Domokos, F. Brennecke, and T. Esslinger, Cold atoms in cavity-generated dynamical optical potentials, *Rev. Mod. Phys.* **85**, 553 (2013).
- [65] P. Hamilton, M. Jaffe, J. M. Brown, L. Maisenbacher, B. Estey, and H. Müller, Atom interferometry in an optical cavity, *Phys. Rev. Lett.* **114**, 100405 (2015).
- [66] D. Yum, D. D. Munshi, T. Dutta, and M. Mukherjee, Optical barium ion qubit, *J. Opt. Soc. Am. B* **34**, 1632 (2017).
- [67] S. Fishman, G. De Chiara, T. Calarco, and G. Morigi, Structural phase transitions in low-dimensional ion crystals, *Phys. Rev. B* **77**, 064111 (2008).
- [68] A. Retzker, R. C. Thompson, D. M. Segal, and M. B. Plenio, Double well potentials and quantum phase transitions in ion traps, *Phys. Rev. Lett.* **101**, 260504 (2008).
- [69] J. D. Baltrusch, C. Cormick, G. De Chiara, T. Calarco, and G. Morigi, Quantum superpositions of crystalline structures, *Phys. Rev. A* **84**, 063821 (2011).
- [70] S. Patsch, D. M. Reich, J.-M. Raimond, M. Brune, S. Gleyzes, and C. P. Koch, Fast and accurate circularization of a Rydberg atom, *Phys. Rev. A* **97**, 053418 (2018).
- [71] A. Bermudez, T. Schaetz, and D. Porras, Synthetic gauge fields for vibrational excitations of trapped ions, *Phys. Rev. Lett.* **107**, 150501 (2011).
- [72] R. Schmied, T. Roscilde, V. Murg, D. Porras, and J. I. Cirac, Quantum phases of trapped ions in an optical lattice, *New J. Phys.* **10**, 045017 (2008).
- [73] S. Fey, S. C. Kapfer, and K. P. Schmidt, Quantum criticality of two-dimensional quantum magnets with long range interactions, *Phys. Rev. Lett.* **122**, 017203 (2019).
- [74] R. Nath, M. Dalmonte, A. W. Glaetzle, P. Zoller, F. Schmidt-Kaler, and R. Gerritsma, Hexagonal plaquette spin-spin interactions and quantum magnetism in a two-dimensional ion crystal, *New J. Phys.* **17**, 065018 (2015).